Title
The impact of ethanol and iso-butanol blends on gaseous and particulate emissions from two passenger cars equipped with spray-guided and wall-guided direct injection SI (spark ignition) engines

Journal
Energy, 82

ISSN
03605442

Authors
Karavalakis, Georgios
Short, Daniel
Vu, Diep
et al.

Publication Date
2015-03-01

DOI
10.1016/j.energy.2015.01.023

Peer reviewed

Energy 82 (2015) 168–179

Contents lists available at ScienceDirect

Energy

journal homepage: www.elsevier.com/locate/energy

The impact of ethanol and iso-butanol blends on gaseous and particulate emissions from two passenger cars equipped with spray-guided and wall-guided direct injection SI (spark ignition) engines

Georgios Karavalakis [a, b, *], Daniel Short [a, b], Diep Vu [a, b], Robert L. Russell [a], Akua Asa-Awuku [a, b], Heejung Jung [a, c], Kent C. Johnson [a, b], Thomas D. Durbin [a, b]

[a] University of California, Bourns College of Engineering, Center for Environmental Research and Technology (CE-CERT), 1084 Columbia Avenue, Riverside, CA 92507, USA
[b] Department of Chemical and Environmental Engineering, Bourns College of Engineering, University of California, Riverside, CA 92521, USA
[c] Department of Mechanical Engineering, Bourns College of Engineering, University of California, Riverside, CA 92521, USA

ARTICLE INFO

Article history:
Received 2 August 2014
Received in revised form
3 December 2014
Accepted 8 January 2015
Available online 7 February 2015

Keywords:
Ethanol
Iso-butanol
Gasoline direct injection
Emissions
Particles
Aldehydes

ABSTRACT

We examined the effects of different ethanol and iso-butanol blends on the gaseous and particulate emissions from two passenger cars equipped with spark ignition direct injection engines and with one spray-guided and one wall-guided configuration. Both vehicles were tested over triplicate FTP (Federal Test Procedure) and UC (Unified Cycles) using a chassis dynamometer. Emissions of THC (total hydrocarbons), NMHC (non-methane hydrocarbons), and CO (carbon monoxide) reduced with increasing oxygen content in the blend for some of the vehicle/fuel combinations, whereas NO_x (nitrogen oxide) emissions did not show strong fuel effects. Formaldehyde and acetaldehyde were the main carbonyls in the exhaust, with the higher ethanol blends showing higher acetaldehyde emissions during the cold-start. For butyraldehyde emissions, both vehicles showed some increases with different butanol blends when compared to ethanol blends, but not for all cases. The higher ethanol and butanol blends showed reductions in PM (particulate mass), number, and soot mass emissions. Particulate emissions were significantly affected by the fuel injection design, with the wall-guided vehicle producing higher mass and number emissions compared to the spray-guided vehicle. Particle size was influenced by ethanol and iso-butanol content, with higher alcohol blends showing lower accumulation mode particles than the baseline fuel.

1. Introduction

The proportion of gasoline vehicles operating with SI (spark ignition) DI (direct injection) fueling systems is steadily increasing in both the European and the U.S. (United States) markets. In the U.S. alone, the widespread penetration of gasoline vehicles with DI engines has increased from 4% in 2009 to 38% in 2014 [1]. The penetration of SIDI vehicles is due to their improved fuel economy over conventional throttled SI PFI (port fuel injection) engines, as direct injection increases thermodynamic efficiency and improves fueling control, and ultimately leads to CO_2(carbon dioxide) reductions [2].

The vast majority of SIDI engines employ wall-guided designs in which the fuel spray is directed from a side-mounted fuel injector towards a contoured piston and then upward toward the spark plug [3]. While wall-guided SIDI (WG-SIDI) engines offer advantages over their PFI counterparts, there can be issues relating to fuel preparation. Fuel contact with the cylinder wall surfaces during combustion leads to the formation of soot or other semi-volatile compounds, because the wall quenches the flame and prevents complete combustion of the fuel [4]. In addition to soot formation, an increase in THC (total hydrocarbon) emissions is expected due to incomplete evaporation and mixing with air and adsorption and

* Corresponding author. University of California, Bourns College of Engineering, Center for Environmental Research and Technology (CE-CERT), 1084 Columbia Avenue, Riverside, CA 92507, USA. Tel.: +1 9517815799; fax: +1 9517815790.
E-mail address: gkaraval@cert.ucr.edu (G. Karavalakis).

http://dx.doi.org/10.1016/j.energy.2015.01.023
0360-5442/

subsequent desorption of the fuel that, after being trapped in the piston top land crevice, is dissolved in lubricant oil, which can lead to dilution of the lubricant oil and loss of its lubricant properties [2–4].

Currently, stoichiometric homogeneous WG-SIDI engines are the dominant share of SIDI vehicles penetrating the market. Alternative designs to WG-SIDI engines use either homogeneous or stratified-charge SG (spray-guided) SIDI engines [5]. While SG-SIDI engines can be operated in a homogeneous charge mode only, the greatest fuel economy benefit is achieved with unthrottled lean stratified operation [6]. Advanced SG-SIDI engines are mostly available in Europe, but not in the U.S. because their lean operation requires nitrogen oxides (NO_x) emissions control [7]. For the SG-SIDI configuration, the fuel injector and spark plug electrodes are close-spaced in the center of the chamber. The fuel injector confines the fuel spray such that it does not contact the cylinder walls, thus reducing the incidence of fuel wall wetting, improving mixing and reducing soot formation [5,7,8].

While SIDI engines offer important fuel economy and CO_2 reduction benefits compared to their PFI counterparts, additional changes are ongoing in the fuel industry to further reduce greenhouse gas emissions and to increase the use of renewable fuels. In the U.S., the passage of the Energy Independence and Security Act (EISA 2007) along with the RFS (Renewable Fuel Standard), which was initiated in 2005 and expanded in 2007, mandates the use of 36 billion gallons of renewable fuels in the transportation fuel pool by 2022 [9]. Analogous to the U.S., the EU (European Union) also promotes the use of renewable fuels with the implementation of the EU Renewable Energy Directive (2009/28/EC), which sets an objective of 10% market share of biomass fuels by 2020 [10]. Currently, ethanol produced both from corn and other cellulosic feedstocks is considered to be the most promising biofuel in the U.S. [11]. However, there are several drawbacks with the use of ethanol as gasoline extender. These include ethanol's lower energy content (26.8 MJ/kg) compared to gasoline (42.7 MJ/kg), the increase in RVP (Reid vapor pressure), and the inability to transport it through pipelines due to risk of water-induced phase separation [12,13].

Recently, higher alcohols, such as butanol, have been the subject of increased interest as potential fuels in SI engines [14]. Butanol is a higher chain alcohol with a four carbon structure that has different isomers based on the location of the hydroxyl group (1-butanol, n-butanol, 2-butanol, tertiary-butanol, and iso-butanol) [15]. While n-butanol could be an attractive candidate for ethanol replacement because it can be produced via the mature and well-known ABE (acetone–butanol–ethanol) fermentation process, the dramatic energy demand, high water use, and unfavorable process economics have led research towards iso-butanol [16]. Similar to ethanol, iso-butanol can be produced from biochemical pathways via fermentation using biomass-derived feedstocks, including corn, sugarcane, and cellulosic biomass [16,17]. Compared to ethanol, butanol exhibits a higher energy density (33.1 MJ/kg), which is close to that of gasoline. In addition, butanol has a lower latent heat of vaporization, is less soluble in water, and less corrosive than ethanol. The motor octane number of butanol is lower than ethanol. However, both butanol and ethanol improve the octane ratings of gasoline when they are added [15,16].

The use of ethanol has been widely investigated for SI engines and vehicles, while data on emissions from butanol blends is relatively sparse. While most studies on the effects of ethanol on tailpipe emissions have been focused on PFI engines and vehicles [18,19], there are some studies available on SIDI engines/vehicles. Storey et al. [20] analyzed the effect of E10 and E20 blends on a 2007 model year SIDI vehicle and found that NO_x, CO (carbon monoxide), formaldehyde, and benzaldehyde emissions decreased with higher ethanol blends, while acetaldehyde emissions showed increases. They also showed reduced PM (particulate mass) mass and particle number emissions with ethanol blends. Maricq et al. [21] showed small benefits in PM mass and particle number emissions as the ethanol level in gasoline increased from 0 to 20% when they tested a SIDI turbocharged vehicle with two engine calibrations over the FTP (Federal Test Procedure); while particle size was unaffected by ethanol level. Chen et al. [22] investigated the effect of ethanol blending on the characteristics of PM and particle number emissions from an SG-SIDI engine. They found increases in particulate emissions as the ethanol content increased. Clairotte et al. [23] showed that a flex fuel vehicle fitted with a SIDI engine reduced CO, CO_2, and NO_x emissions with higher ethanol blends. However, the same study showed higher emissions of THC, NMHC (non-methane hydrocarbons), formaldehyde, and acetaldehyde with increasing ethanol content. Higher THC emissions with higher ethanol blends were also seen in other studies employing SG-SIDI engines [24]. In addition, Graham et al. [25] showed lower CO and NMOG (non-methane organic gases) emissions from a SIDI vehicle with E10 and E20 blends relative to gasoline. They also showed increases in formaldehyde, 1,3-butadiene, and benzene emissions with ethanol use.

Most chassis dynamometer studies on butanol blends have been conducted on PFI-fueled vehicles [26,27]. Recent engine investigations on butanol blends on WG-SIDI engines have shown that NO_x, CO, and THC emissions were lower with increasing butanol content in gasoline, while some increases were seen for formaldehyde and acetaldehyde emissions when they utilized n-butanol and iso-butanol as blending agents with gasoline [28]. In another study, the same group of authors showed lower volumetric fuel consumption and lower NO_x emissions for butanol compared to ethanol blends [29]. Finally, Karavalakis et al. [30] studied the gaseous and particulate emission effects of different ethanol and iso-butanol blends from a fleet of PFI and WG-SIDI vehicles over the FTP and UC (Unified Cycle). Their results did not show strong differences between fuels for THC, CO, and NO_x emissions for either of the cycles. They showed higher PM mass, particle number, and black carbon emissions for the DI vehicles compared to their PFI counterparts. They also showed reductions in PM mass, particle number, and black carbon emissions with increasing alcohol content.

In this study, the impacts of varying ethanol and iso-butanol blend concentrations on the tailpipe emissions from two passenger cars equipped with SG-SIDI and WG-SIDI fueling systems, respectively, are evaluated. Emissions and fuel economy testing was conducted over the FTP and the UC (Unified Cycle) test cycles that include both cold-starts and transient operation. A major goal of this study was to investigate the influence of fuel type and engine technology on particle emissions, including PM mass, particle number, soot, and particle size distributions and HAPs (hazardous air pollutants), such as carbonyl compounds and monoaromatic volatile organic compounds.

2. Experimental procedure

2.1. Test fuels and vehicles

Six fuels were employed in this study. The fuel test matrix included an E10 fuel (10% ethanol and 90% gasoline), which served as the reference fuel for this study, and two additional ethanol blends, namely E15 and E20. Iso-butanol, which is a branched isomer of butanol with the OH group at the terminal carbon, was blended with gasoline at proportions of 16% (Bu16), 24% (Bu24), and 32% (Bu32) by volume, which is the equivalent of E10, E15, and E20, respectively, based on the oxygen content. All fuels were custom blended to match the oxygen contents, maintain the RVP

within certain limits (6.4–7.2 psi), and match the fuel volatility properties. The main fuel parameters of the alcohol blends can be found elsewhere [30].

This study utilized two 2012 model year gasoline passenger cars fitted with three-way catalysts (TWC) and operated stoichiometrically. The first vehicle (WG-SIDI) was a 2.0L, California LEVII, SULEV certified passenger car, having a rated horsepower of 148 hp at 6500 rpm, and equipped with a wall-guided direct injection SI engine. The second vehicle (SG-SIDI) was a 3.5L, California LEVII, SULEV certified passenger car, having a rated horsepower of 302 hp at 6500 rpm, and equipped with a spray-guided direct injection SI engine. The cars had accumulated mileages of 18,851 and 10,996 miles, respectively, at the beginning of the test campaign.

2.2. Driving cycles and measurement protocol

Each vehicle was tested on each fuel over three FTPs and three UC tests. The six tests on a particular fuel were conducted sequentially once the vehicle was changed to operate on that fuel, and the fuel was not changed to another fuel during this time. A fuel change with multiple drain and fills was conducted between the testing on each fuel to condition the vehicle and ensure no carry-over effects. A schematic on the fuel preconditioning procedure is given in Figure S1 (Supplementary Material). Detailed information on the driving cycles employed in this study and the testing protocol can be found elsewhere [31].

2.3. Emission testing and analysis

All tests were conducted in CE-CERT's VERL (Vehicle Emissions Research Laboratory), which is equipped with a Burke E. Porter 48-inch single-roll electric dynamometer. A Pierburg PDP-CVS (Positive Displacement Pump-Constant Volume Sampling) system was used to obtain certification-quality emissions measurements. For all tests, standard bag measurements were obtained for THC, CO, NO_x, NMHC, and CO_2. NMHC was determined from the combined results from the THC analyzer and a separate CH_4 (methane) analyzer. Bag measurements were made with a Pierburg AMA-4000 bench.

Samples for carbonyl analysis were collected on 2,4-dinitrophenylhydrazine (DNPH) coated silica cartridges (Waters Corp., Milford, MA) and subsequently analyzed using an Agilent 1200 series HPLC (high performance liquid chromatography) equipped with a variable wavelength detector. Samples for 1,3-butadiene, benzene, toluene, ethylbenzene, and xylenes were collected using Carbotrap adsorption tubes consisting of multi-beds, including a molecular sieve, activated charcoal, and carbotrap resin. An Agilent 6890 GC with a FID maintained at 300 °C was used to measure the volatile organic compounds. Detailed information on the method used to collect and analyze the carbonyl compounds and 1,3-butadiene, benzene, toluene, ethylbenzene, and xylene compounds can be found elsewhere [18].

PM measurements were made on both a mass and number basis. PM mass samples were collected cumulatively over the entire length of the FTP and UC cycles, with one sample collected for each test. Total PM mass samples were collected using 47 mm Teflon® filters and weighed with a 1065-compliant microbalance in a temperature and humidity controlled clean chamber. Total particle number was measured using a TSI 3776 ultrafine-CPC (Condensation Particle Counter) with a 2.5 nm cut point. An ejector diluter was used to collect samples from the CVS tunnel. Real-time particle size distributions were also obtained for some fuel blends using an EEPS (Engine Exhaust Particle Sizer) spectrometer (TSI 3090, firmware version 8.0.0). The EEPS was used to obtain real-time second-by-second size distributions between 5.6 and 560 nm. Real-time soot emissions were measured using an AVL MSS (Micro-Soot Sensor).

2.4. Statistical analysis

The statistical program Systat 13 was used to analyze the data for statistically significant fuel effects. Statistical analyses were run on the combined data sets from both vehicles. A natural logarithmic transformation of the data was employed to make the distribution of the residuals normal. A mixed model with fuels as the fixed factor and vehicles as the random factor was employed. This model uses the REML (Residual or Restricted Maximum Likelihood) method to determine if there are statistically significant fuel effects for a given emission in at least one of the fuel groups. Because there are six fuels it is necessary to perform a pairwise comparison test to determine which fuels have statistically significant emission differences. The program provides six pairwise tests and recommends the Bonferroni test for small datasets. The Bonferroni pairwise comparison test with a confidence level of 95% was used to identify which fuels had statistically different emissions. The program provides the actual p value (a value between 0 and 1, where 0.05 is the 95% confidence level that the emissions are statistically different) for each fuel versus each other fuel. In this study, any differences which have a % confidence level of $\geq$95% are considered statistically significant and any differences with % confidence levels between 90% and <95% are considered marginally statistically significant.

3. Results and discussion

The weighted FTP and UC emissions and fuel economy results for the testing of two vehicles are presented in the following figures. The results for each vehicle/fuel combination represent the average of all test runs on that particular combination. The error bars represent one standard deviation on the average values for each fuel.

3.1. Regulated emissions and fuel economy

The THC emission results for the SG-SIDI and the WG-SIDI vehicles over the FTP and UC test cycles are presented in Fig. 1a. Overall, THC emissions were found to be at relatively low levels for both vehicles, ranging from 0.008 to 0.016 g/mile for the FTP and 0.008 to 0.022 g/mile for the UC. Generally, the higher ethanol blends exhibited lower THC emissions for the SG-SIDI vehicle, while no strong fuel trends were observed for the butanol blends for the SG-SIDI vehicle or for the WG-SIDI vehicle. The decreases in THC emissions are ascribed to the fuel-bound oxygen [32]. For the FTP, THC emissions did not show any statistically significant differences for the weighted, hot-running, and hot-start phases of the cycle. For the cold-start phase of the FTP, THC emissions showed a marginally statistically significant reduction of 31% for E20 compared to Bu24. Similar to the FTP, the THC emissions did not show any statistically significant differences for the UC with the exception of cold-start emissions. For the cold-start phase, THC emissions showed a statistically significant reduction of 40% for E20 compared to Bu24.

The majority of THC emissions were emitted during the first 200–300 s of the cold-start phase of the FTP and UC. For the FTP, the average cold-start THC emissions ranged from 0.033 to 0.055 g/mile for the SG-SIDI vehicle and 0.029 to 0.040 g/mile for the WG-SIDI vehicle. For the UC, the average cold-start THC emissions ranged from 0.100 to 0.162 g/mile for the SG-SIDI vehicle and 0.082 to 0.122 g/mile for the WG-SIDI vehicle. The higher cold-start THC emissions are due to the TWC being below its light-off operating

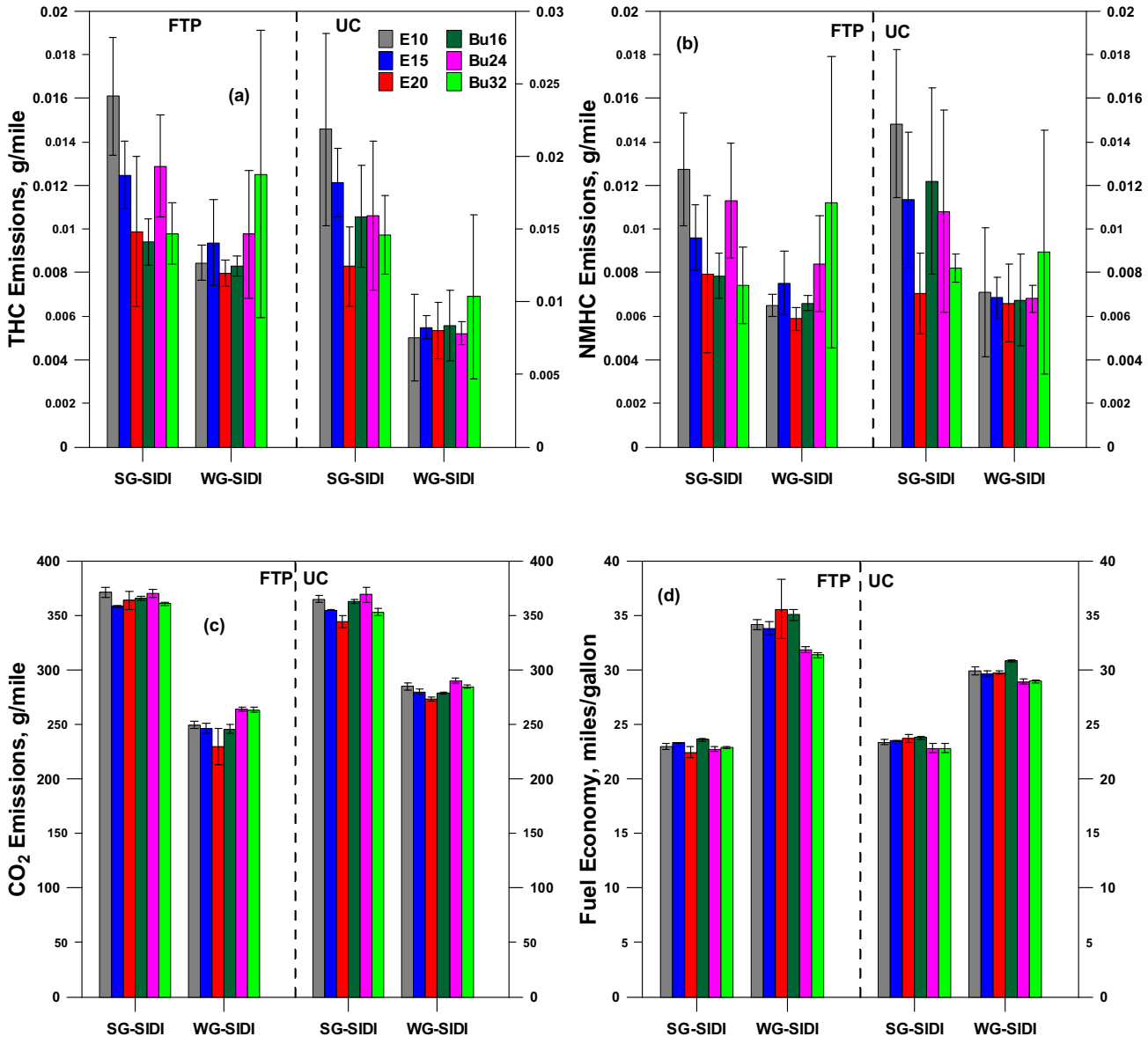

Fig. 1. (a–d): THC (top panel, a), NMHC (top panel, b), CO_2 (bottom panel, c) emissions, and fuel economy (bottom panel, d) for the SG-SIDI and WG-SIDI vehicles over the FTP and UC cycles as a function of fuel type.

temperature. THC emissions for the hot-running and hot-start phases were practically eliminated due to the efficient oxidation of hydrocarbons by the TWC. Fuel impingement effects can also significantly influence THC emissions in SIDI engines [3], especially during cold-start conditions, where THC emissions could be a result of unburned fuel fractions. It is assumed that increased cylinder surface temperatures also contribute to lower THC emissions during the hot-running and hot-start phases by aiding better fuel vaporization and minimizing pool fires.

The weighted NMHC emissions, presented in Fig. 1b, did not show any statistically significant differences between the fuels for the two vehicles combined. NMHC emissions for the cold-start showed statistically significant reductions of 35% and 42% for E20 compared to Bu24 for the FTP and UC, respectively. For the FTP, NMHC emissions for the hot-running phase both increased and decreased at a marginally statistically significant level for E10 compared to E20 and E20 compared to Bu24, respectively.

Fig. 1c shows the effect of alcohol fuel formulation on the CO_2 emissions over the FTP and UC for both vehicles. From a theoretical standpoint, it might be expected that CO_2 emissions would trend with the carbon/hydrogen ratio in the fuel. Carbon/hydrogen ratio decreases in the following order E10/Bu16, E15/Bu24, and E20/Bu32. Although some differences are seen between different fuels for different vehicles/cycles, there is not a general trend of CO_2 increases seen with that fuel order for these two different vehicles. For the FTP, the weighted CO_2 emissions showed statistically significant reductions of 8% for E20 compared to Bu24 for both vehicles. For the UC, the differences between the fuels were more pronounced with E20 and Bu24 producing statistically significant increases of 4% and 3%, respectively, compared to E10 and Bu32. Overall, Bu24 showed the highest weighted CO_2 emissions, with E15 and E20 showing statistically significant reductions of 4% and 5%, respectively, compared to the Bu24 blend, while a marginally statistically significant reduction of 3% for Bu16 compared to Bu24

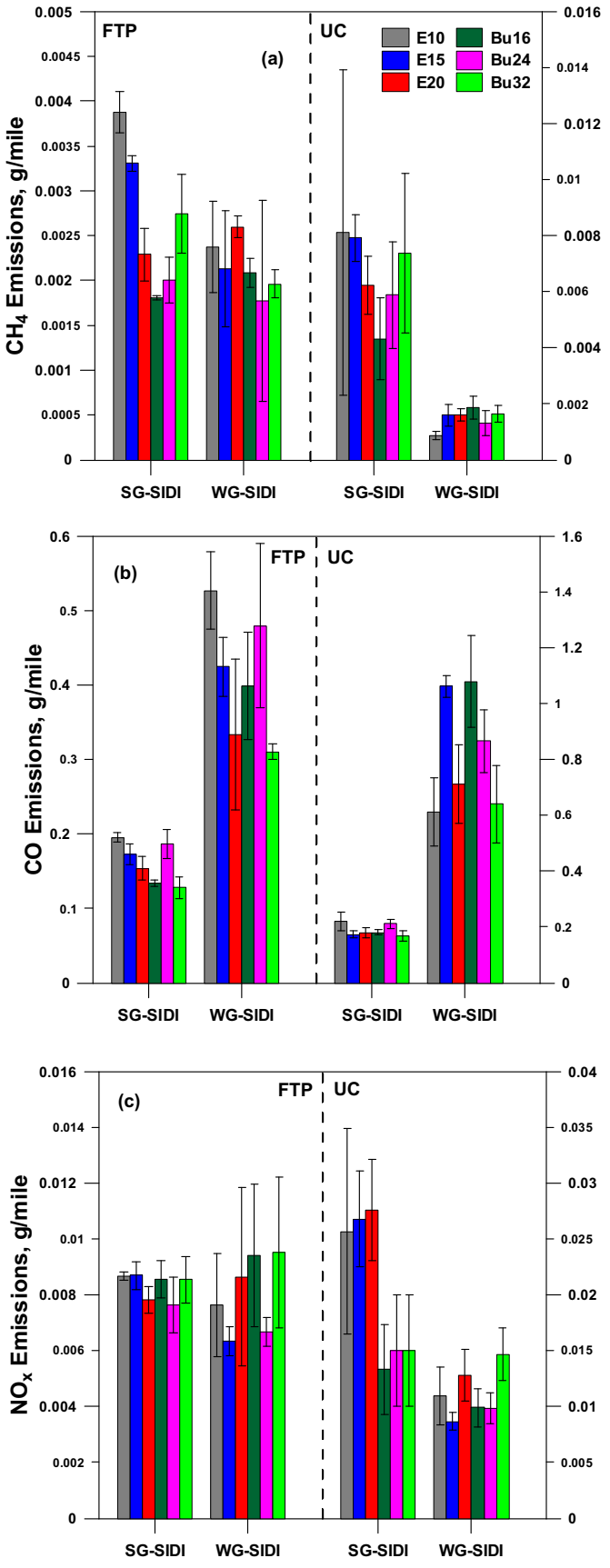

Fig. 2. (a–c): CH_4 (a), CO (b), and NO_x (c) emissions for the SG-SIDI and WG-SIDI vehicles over the FTP and UC cycles as a function of fuel type.

was also seen. For both test cycles, cold-start CO_2 emissions showed statistically significant reductions of 9% for both the FTP and the UC with E20 compared to Bu24. For the FTP hot-running phase CO_2 emissions, the lowest emissions were seen for E20, which showed statistically significant or marginally statistically significant reductions of 4%–6% relative to the Bu24, Bu32, and E10 blends. For the UC hot-running CO_2 emissions, Bu24 showed the highest emissions with E10, E20, and Bu16 showing statistically significantly or marginally statistically significant reductions of 3%–5% compared to the Bu24 blend. E20 also showed a decrease of 4% compared to E10 at a statistically significant level. During the hot-start for the FTP, CO_2 emissions for E20 showed a statistically significant decrease of 10% relative to Bu24, whereas no statistical differences were seen between the fuels for the UC.

Fuel economy for each vehicle/fuel combination is presented in Fig. 1d. Fuel economy was calculated based on the carbon balance method and the unique properties for each different fuel. There were some trends of fuel economy reductions with increasing alcohol content/energy content, but not in all cases. The butanol fuels showed the most significant fuel economy differences. For the FTP, weighted fuel economy results showed statistically significant increases of 7% for Bu16 compared to Bu24 and Bu32, respectively. Statistically significant increases with Bu16 of 5% and 6% for the hot-running phase and 9% and 8% for the hot-start phase compared to Bu24 and Bu32, respectively, were also observed. For the UC, weighted fuel economy showed statistically significant increases of 5% and 4% for Bu16 relative to Bu24 and Bu32, respectively. On the other hand, there were no statistically significant differences between the fuel economies for the different ethanol fuels. The ethanol fuels did show some statistically significant differences compared to some of the butanol fuels and generally showed higher fuel economies than the Bu24 and Bu32 fuels.

Emissions of CH_4 are a function of the type of fuel used, the design and tuning of the engine, the type of emission control system, the age of the vehicle, as well as other factors [33]. Generally, CH_4 emissions from gasoline are relatively small in terms of global warming potential. As shown in Fig. 2a, CH_4 emissions were found at very low levels ranging from 0.0017 to 0.004 g/mile for the FTP and 0.0008 to 0.008 g/mile for the UC, with the SG-SIDI vehicle having higher CH_4 emissions compared to the WG-SIDI vehicle over both cycles. Note that if the CH_4 emissions are multiplied by CO_2 equivalent global warming potential factor 21 that CH_4 emissions contributed significantly less to the global warming potential of the exhaust compared to CO_2 emissions. For the SG-SIDI vehicle, some trends towards lower CH_4 emissions with E15 and E20 blends relative to E10 and higher CH_4 emissions with Bu24 and Bu32 relative to Bu16 were seen for both cycles. On the other hand, the WG-SIDI vehicle did not show consistent fuel trends. In general, the precursors of CH_4 formation are CH_3 and C_8H_{18}, which suggests that the addition of either ethanol or butanol to gasoline could inhibit the path via C_8H_{18} decomposition to produce CH_4 [34]. The cold-start CH_4 emissions for the FTP showed statistically significant differences between fuels, with E20, Bu16, Bu24, and Bu32 showing decreases of 48%, 65%, 49%, and 50%, respectively, compared to E10. For the FTP, further statistically significant increases of 49% for E20 compared to Bu24 were seen over the hot-start phase. No statistically significant differences between the fuels were observed for the UC. Cold-start CH_4 emissions were found to be somewhat higher compared to hot-running and hot-start phases for both cycles. The differences in CH_4 emissions between the cold and warm phases of the FTP and UC tests were not as pronounced as those found for THC and NMHC. This was probably due to the fact that CH_4 is a more inert gas in terms of its oxidation activity in the TWC. So, the reductions in CH_4 emissions during the hot-running and hot-start phases due to activation and light-off of the TWC are not as significant as the corresponding reductions seen for the THC and NMHC emissions.

CO emissions are shown in Fig. 2b. CO emissions ranged from 0.134 to 0.527 g/mile for the FTP and 0.168 to 1.080 g/mile for the UC, with the SG-SIDI vehicle producing considerably lower CO emissions than the WG-SIDI vehicle. For the FTP, weighted CO emissions showed statistically significant decreases of 37%, 33%, and 48%, respectively, for E20, Bu16, and Bu32 compared to E10. The intermediate Bu24 blend showed emissions that were higher at a statistically significant level than those of E20, Bu16, and Bu32. For the cold-start CO emissions, E10 was higher at a statistically significantly level on the order of 41% and 54%, respectively, compared to E20 and Bu32, and marginally statistically significantly higher on the order of 33% compared to Bu16. Additionally, Bu24 showed a 37% increase relative to Bu32 at a statistically significant level. For the hot-start phase of the FTP, CO emissions showed statistically significant increases of 44% and 46%, respectively, for E10 and E15 compared to the Bu32 blend. No strong trends between the test fuels for the weighted CO emissions were seen for the UC. For the cold-start CO emissions, E10 showed a marginally statistically significant decrease of 41% and a statistically significant decrease of 45% compared to Bu16 and Bu24, respectively. A marginally statistically significant decrease of 39% was also seen for E20 compared to Bu24.

There were some trends of lower CO emissions with the higher alcohol fuel blends for both vehicles, with some exceptions. This trend was stronger for the ethanol blends, whereas the intermediate Bu24 tended to show the highest emissions for the butanol blends. Previous studies have shown reductions in CO with increasing alcohol content due to improved oxidation of the CO as a result of the oxygen content in the fuel [18,32,35]. It was observed that the higher CO reductions were achieved with E20 and Bu32 blends relative to E10. While it is hypothesized that the oxygen content was the primary contributing factor for the CO decrease, it might be possible that the CO decreases with E20 could also be a result of its considerably lower 50% distillation temperature (T50) compared to the other blends. This is in agreement with a previous study conducted by Durbin et al. [19] where they found reduced CO emissions with lower T50 in ethanol blends. This is also in agreement with the findings of the EPAct study, which showed that both a combination of fuel-borne oxygen and lower T50 were responsible for lower CO emissions on a fleet of PFI vehicles when running on ethanol blends [36]. It should be emphasized that similar to THC/NMHC emissions, CO emissions were dominated by the cold-start portion of the FTP and UC, largely due to the catalyst being below its light-off temperature.

NO_x emissions as a function of fuel type are presented in Fig. 2c. NO_x emissions ranged from 0.006 to 0.010 g/mile for the FTP and from 0.009 to 0.028 g/mile for the UC. The NO_x emissions for the two vehicles were comparable over the FTP, but were higher for the SG-SIDI vehicle on ethanol blends compared to butanol blends and compared to the WG-SIDI vehicle over the UC. Overall, NO_x emissions did not show any consistent fuel trends or any statistically significant differences between fuels for the FTP and UC. Interestingly, some differences between the fuels were only observed for the hot-start phase of both the FTP and UC. For the FTP, E10 and E15 showed statistically significant NO_x decreases of 65% and 67%, respectively, compared to Bu32. For the UC, NO_x emissions showed statistically significant decreases of 96% and 101%, respectively, for E15 compared to E20 and Bu32.

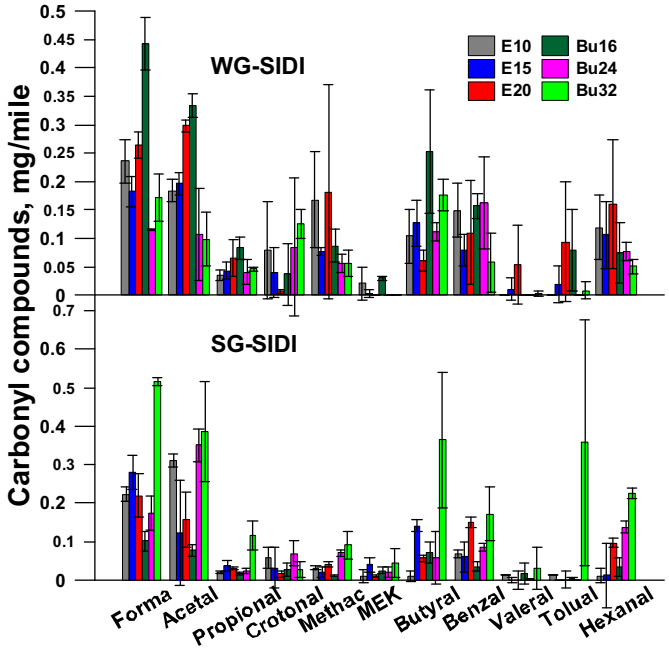

Fig. 3. Carbonyl emissions for both vehicles over the FTP cycle.

3.2. Hazardous air pollutants

3.2.1. Carbonyl emissions

Carbonyl compounds are displayed in Fig. 3 for the SG-SIDI and WG-SIDI vehicles over the FTP as a function of fuel type. Carbonyl emissions were only measured over the FTP cycle. A total of eleven aldehydes and ketones were identified and quantified in the tailpipe for both vehicles, with low molecular-weight aldehydes, such as formaldehyde and acetaldehyde, being the most abundant compounds followed by butyraldehyde, benzaldehyde, propionaldehyde, crotonaldehyde, methacrolein, and hexanaldehyde. In general, carbonyl emissions did not show consistent trends between the fuels and vehicles over the FTP. For formaldehyde emissions, the higher ethanol blends did not show any statistical differences when compared to E10. Most butanol blends trended lower than E10, although not at a statistically significant level and in both vehicles one of the butanol blends showed the highest formaldehyde emissions. Previous studies have shown that alcohol fuels are usually prone to form aldehydes, with some studies showing that iso-butanol blends produced higher formaldehyde emissions than ethanol blends [18,26–28,37]. For iso-butanol, formaldehyde is produced through the oxidation of methyl radicals to form CH_3O and hydroxyl radicals that in turn yield formaldehyde. Formaldehyde is also formed by β-scission decomposition of the C_4H_8OH radical [34,38].

For weighted acetaldehyde emissions, there were no strong fuel trends, although E20 showed a marginally statistically significant increase of 61% compared to Bu24. For acetaldehyde emissions, the fuel influence was more pronounced during the cold-start of the FTP. Increases at a statistically significant level for E20 on the order of 154%, 187%, 228%, and 155%, respectively, were seen relative to E10, Bu16, Bu24, and Bu32 blends. E15 also showed a statistically significant increase of 164% relative to Bu24 and a marginally statistically significant increase of 131% relative to Bu16. Ethanol's effects on acetaldehyde emissions are well understood, and the ethanol blends results reported here, at least for the cold-start, were as expected. Acetaldehyde is principally formed due to the partial oxidation of ethanol, which explains the tendency for acetaldehyde to increase with ethanol concentration [39]. The lack of trends for acetaldehyde with ethanol content for the non-cold-start portions of the cycle could be attributed to the high efficiency of the TWC once it reaches its light-off temperature. Iso-butanol can also form acetaldehyde through the C–C bond scission reaction of iso-butanol and hydrogen atom abstraction from iso-butanol to produce C_4H_8OH radical, which further undergoes β-

scission [40]. This formation pathway is not as strong as that for ethanol, however.

Butyraldehyde emissions exhibited mixed results for both vehicles, with the SG-SIDI and the WG-SIDI vehicles showing increases and decreases for the higher ethanol blends relative to E10, respectively. Both vehicles showed increases in butyraldehyde emissions with the butanol blends when compared to ethanol blends, but not for all cases. The impact of iso-butanol blending on butyraldehyde emissions was particularly strong with Bu32 showing statistically significant increases of 229%, 186%, and 650% compared to E10, E15, and E20 blends. Further statistically significant increases were observed for Bu16 (294%) and Bu24 (331%) relative to E20. For the cold-start phase of the FTP, Bu32 showed statistically significant increases in butyraldehyde emissions of 492% and 553%, respectively, compared to E10 and E15 blends. A marginally statistically significant increase of 254% was also seen for Bu24 relative to E15. Butyraldehyde is expected as a combustion product from iso-butanol blends, with the results reported here being in agreement with those reported in recent studies by Ratcliff et al. [27] and Karavalakis et al. [30]. It was hypothesized that butyraldehyde was produced via sequential H-atoms abstractions from the iso-butanol hydroxyl moiety to form a C_4H_9O radical, which then undergoes β-scission to yield butyraldehyde [41].

Propionaldehyde emissions showed some statistically significant increases during the cold-start phase of the FTP cycle for Bu32, which was higher on the order of 292%, 292%, and 197%, respectively, relative to E10, E15, and E20. Exhaust propionaldehyde is primarily produced from straight-chain hydrocarbons and tends to decrease with increasing fuel aromatics [39], although this trend was not seen in the current study. For the butanol blends, propionaldehyde is mainly formed from 1-propenol via H and/or HO_2 assisted enol-keto isomerization [38]. Crotonaldehyde emissions did not show strong trends for either ethanol or butanol. The only marginally statistically significant difference was seen for the hot-start phase for E10, which increased on the order of 363% relative to Bu16. The WG-SIDI vehicle did not show any strong effects on methacrolein emissions, while the SG-SIDI vehicle showed some increases for the higher butanol blends compared to E10, with these differences not being statistically significant for the weighted methacrolein emissions or the individual FTP phases. Benzaldehyde emissions, which are formed from fuel aromatic hydrocarbons [39], also showed mixed results for all vehicle/fuel combinations, with both increases and decreases for the higher ethanol and butanol blends relative to E10. At first sight, benzaldehyde emissions for the WG-SIDI vehicle trended lower for the higher alcohol/lower aromatic content blends compared to E10 and Bu16, whereas for the SG-SIDI vehicle, some higher alcohol/low aromatic content blends led to increases in benzaldehyde emissions compared to E10 and Bu16. A more detailed statistical analysis revealed that there were no statistically significant fuel effects for weighted, cold-start, and hot-running benzaldehyde emissions over the FTP.

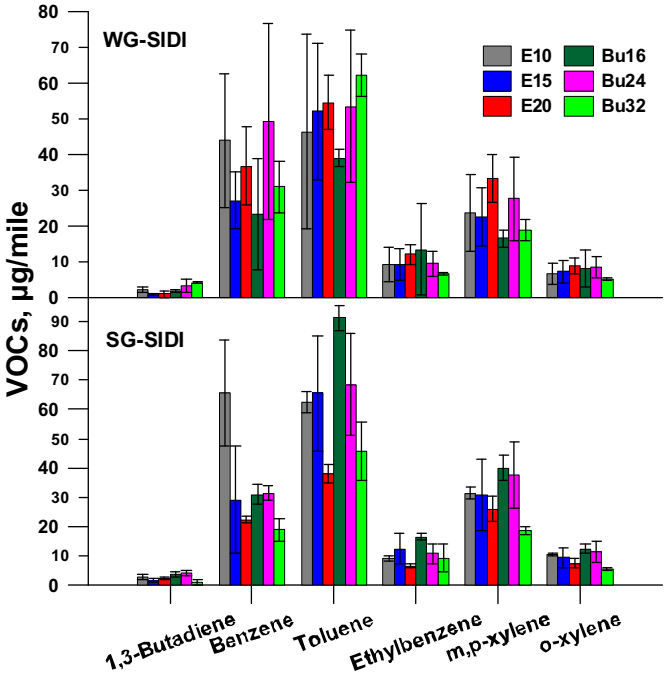

Fig. 4. BTEX and 1,3-butadiene emissions for the SIDI vehicles over the FTP cycle.

3.2.2. BTEX and 1,3-butadiene emissions

Fig. 4 presents the cumulative 1,3-butadiene, benzene, ethylbenzene, toluene, *m/p*-xylene, and *o*-xylene emissions for the WG-SIDI and SG-SIDI vehicles over the FTP. Similar to carbonyl emissions, these pollutants were measured solely for the FTP. The aromatic hydrocarbons of benzene, ethylbenzene, toluene, *m/p*-xylene, and *o*-xylene are commonly referred to as BTEX. For both vehicles, toluene was the principal monoaromatic hydrocarbon followed by benzene and *m/p*-xylene. Emissions of 1,3-butadiene, which is a classified carcinogenic compound to humans, were found at relatively low levels when compared to the BTEX species. Some trends towards lower 1,3-butadiene emissions for the higher ethanol blends and some marginal increases for the butanol blends relative to E10 were seen. The differences in cumulative 1,3-butadiene emissions between the test fuels were not statistically significant, however. For the cold-start phase of the FTP, Bu24 showed a statistically and a marginally statistically significant increase of 157% and 86%, respectively, compared to the E20 and Bu16 blends. For iso-butanol, 1,3-butadiene can be formed from reactions with propargyl or vinyl radicals with ethane, or from the decomposition of the fuel itself.

For benzene emissions, whose principal source is partial combustion of toluene and xylene, some trends towards lower emissions were seen for the higher ethanol blends and butanol blends relative to E10. This phenomenon was more profound for the SG-SIDI vehicle. Statistical analysis for the cycle-composite benzene emissions showed weak fuel effects, with the only statistically significant difference being for Bu16, which showed a decrease of 104% compared to E10. Cumulative toluene emissions did not show a statistically significant fuel effect, while for the cold-start phase Bu24 showed a marginally statistically significant increase of 64% compared to E20. For the hot-start phase, Bu16 showed a marginally statistically significant increase of 347% compared to Bu32. Ethylbenzene emissions did not show a strong fuel influence, with the only statistically significant difference being an apparent 762% increase for Bu16 relative to Bu24 for the hot-running phase of the FTP. Cycle-composite *m/p*-xylene and *o*-xylene emissions were not affected by the fuel blends. However, the cold-start phase showed some fuel differences for *m/p*-xylene emissions for the butanol blends, with Bu24 showing statistical significant increases of 57% and 103%, respectively, relative to Bu16 and Bu32. For the hot-running phase and the hot-start phase, Bu16 showed marginally statistically significant and statistically significant increases of 476% and 300%, respectively, relative to Bu24. For *o*-xylene, Bu24 showed a statistically significant increase of 119% compared to Bu32 over the cold-start phase.

3.2.3. Ozone forming potential and specific reactivity

Non-oxygenated VOCs (volatile organic compounds) and carbonyl compounds are not only known to have direct adverse

health effects, but also affect the environment and have ozone forming potential [42]. To assess the potential of these emissions to produce photochemical ozone, the ozone forming potential using the MIR (maximum incremental reactivity) scale developed by Carter in 2010 [43] was calculated for each fuel/vehicle combination. For the present test conditions, the ozone forming potential was calculated for the BTEX and 1,3-butadiene, carbonyl compounds, CO, and CH_4 emissions over the FTP cycle. As shown in Fig. 5, the highest ozone forming potential was observed for the WG-SIDI vehicle. This was due to the higher mass of CO emissions and high-molecular chain carbonyls found in the tailpipe when compared to the SG-SIDI vehicle, even though the SG-SIDI vehicle produced higher masses of THC, C_2 carbonyls (i.e., formaldehyde and acetaldehyde), and non-oxygenated VOCs emissions.

The fuel effect in ozone forming potential was particularly noticeable for both vehicles, with the majority of the higher ethanol blends and different butanol blends, depending on the vehicle, showing reductions on the ozone precursor emissions relative to E10. It should be stressed that Bu24 and Bu32 blends were found to be more reactive in terms of forming ozone when compared to their oxygen-equivalent E15 and E20 blends, with the exception of the E20 and Bu32 pair for the WG-SIDI. Table S1 (Supplementary Material) shows the ozone forming potential for the alcohol blends for each individual phase of the FTP cycle solely based on the carbonyl compounds. For both vehicles, the cold-start phase showed higher ozone precursor emissions compared to the hot-running and hot-start phases. In most cases, during cold-start conditions, the use of higher ethanol and butanol blends exhibited higher ozone precursor emissions than E10. This result suggests that high alcohol content blends have the potential to increase photochemical ozone during cold-start operation and when the catalyst is not functioning efficiently.

3.2.4. PM mass, soot mass, and particle number emissions

The cycle-based PM mass emissions are shown in Fig. 6a. PM emissions for the WG-SIDI vehicle were considerably higher than those of the SG-SIDI vehicle. For the WG-SIDI vehicle, PM emissions ranged from 1.23 to 2.74 mg/mile for the FTP and from 0.68 to 2.53 mg/mile for the UC, while for the SG-SIDI vehicle PM emissions ranged from 0.09 to 0.38 mg/mile for the FTP and from 0.17 to 0.45 mg/mile for the UC. Lower PM emissions have been found in previous chassis dynamometer studies utilizing SG-SIDI vehicles compared to WG-SIDI vehicles [44,45]. This study showed that PM emissions from SG-SIDI and WG-SIDI engines are significantly different. The lower PM emissions from a spray-guided system are due to the fuel injection architecture, with an injector located close to the spark plug thereby providing better mixture preparation and more efficient fuel evaporation, and less fuel on the floor of the piston bowl [46]. Our results showed that both SIDI vehicles can potentially meet the future California LEV III and Tier 3 standards for PM mass emissions to be implemented by 2017 (3 mg/mile), with the SG-SIDI vehicle even complying with the ultra-low PM standard of 1 mg/mile, which is expected in 2025.

Statistical analysis of the results showed that there were no strong fuel effects on the cycle-based PM emissions for either the FTP or the UC. This result is probably due to the minor differences between the fuels for the SG-SIDI vehicles for both test cycles and somewhat opposite effects for ethanol for the two vehicles, which ultimately influenced the fleet-based statistics. It is worth mentioning that for the SG-SIDI vehicle, a trend towards higher PM emissions for E15 and E20 relative to E10 was seen, however. Similar to the results reported here, Chen et al. [22] showed an increase in PM emissions with increasing ethanol content on a SG-SIDI engine. They attributed these phenomena to the higher enthalpy of vaporization and lower energy density of ethanol, and the poor spray atomization performance for the ethanol blends, which will produce a greater mixture in-homogeneity and induce high PM emissions. For the WG-SIDI vehicle, the use of increasing alcohol content resulted in lower PM emissions, indicating that the oxygen content was the primary factor for reducing PM. The lower PM emissions with alcohol fuels in context with the influence of the oxygen content have been discussed in previous studies [20,21,47].

Fig. 6b shows the soot mass emission results for the SG-SIDI and WG-SIDI vehicles. Note that the MSS instrument was not available

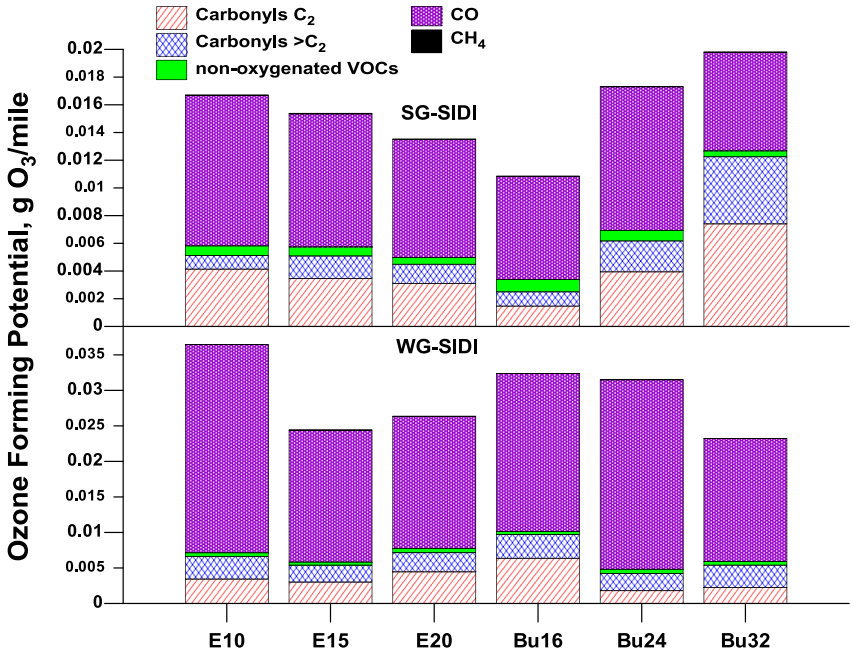

Fig. 5. Ozone formation potential for the ethanol and iso-butanol blends from the SG-SIDI and WG-SIDI vehicles over the FTP cycle.

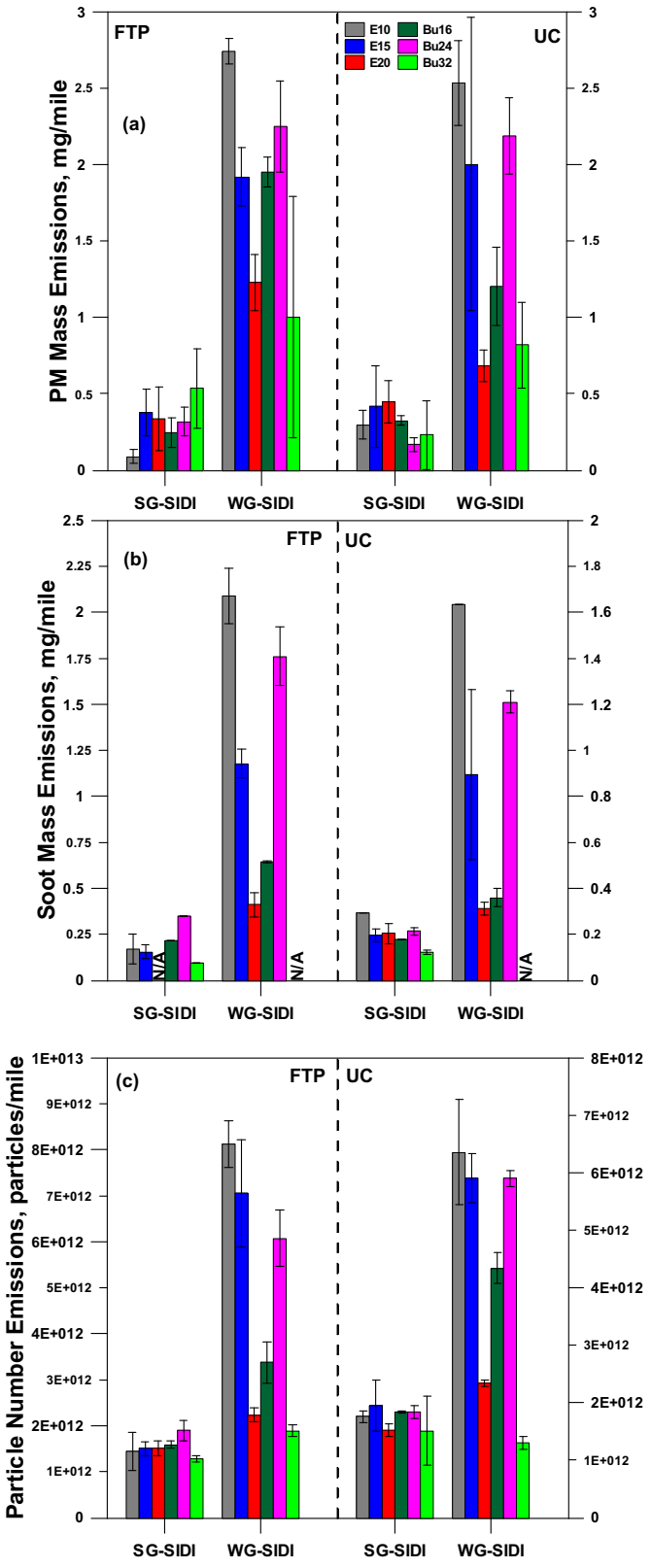

Fig. 6. (a–c): PM mass (a), soot mass (b), and particle number (c) emissions for the SG-SIDI and WG-SIDI vehicles over the FTP and UC cycles as a function of fuel type.

for Bu32 for the WG-SIDI vehicle for both cycles and for E20 for the SG-SIDI for the FTP. For the WG-SIDI vehicle, soot emissions agreed well with the filter-based PM mass and particle number emissions. For the SG-SIDI vehicle, no correlation was seen between soot and PM mass emissions, however. Overall, soot emissions decreased with E15, E20, and Bu16 for the WG-SIDI vehicle at a statistically significant level compared to E10 for both cycles. The intermediate Bu24 blend showed some statistically significant increases in soot emissions compared to Bu16 and also showed lower emissions relative to E10. For the SG-SIDI vehicle, the fuel effect on soot emissions was not consistent, except for the lower Bu32 soot emissions over both cycles. Overall, the lower soot emissions for the higher ethanol blends could be ascribed to the increased oxygen content in the blends, which facilitates a more complete combustion [48]. Coefficients of statistical determination (R^2) showed strong correlations between soot mass emissions and PM mass and particle number emissions for the WG-SIDI vehicle, but not for the SG-SIDI vehicle. For the FTP, soot mass for the WG-SIDI vehicle significantly correlated with PM mass ($R^2 = 0.83$) and particle number ($R^2 = 0.81$). Similarly, for the UC, soot mass highly correlated with PM mass ($R^2 = 0.90$) and particle number ($R^2 = 0.72$).

Particle number emissions are presented in Fig. 6c. In general, particle number emissions agree well with the PM mass trends, with the WG-SIDI vehicle showing higher particle number emissions compared to the SG-SIDI vehicle. Further analysis showed that PM mass emissions were highly correlated to particle number emissions for the WG-SIDI vehicle, but not for SG-SIDI vehicle. The highest correlation was observed for the UC ($R^2 = 0.88$), followed by the FTP ($R^2 = 0.78$). Zhang and McMahon [45] also reported higher particle number emissions for WG-SIDI vehicles compared to SG-SIDI vehicles over the FTP. Note that both vehicles produced higher particle number counts for the higher speed and load UC compared to the FTP. The higher particle number emissions for the WG-SIDI vehicle were likely due to the increasing wall wetting by fuel on the piston, valve, and cylinder liner. This may result in liquid fuel that is not totally vaporized at the start of combustion. As a consequence, local fuel-rich combustion or even pool fires can occur near the piston, generating high particle emissions [49,50]. For the SG-SIDI vehicle, the lower particle number emissions were most likely due to the reduced contact between fuel and combustion chamber surfaces, which was achieved through the higher fuel pressure and therefore better spray atomization and mixture preparation.

Fuel effects were particularly noticeable for both cycles in particle number emissions, with the WG-SIDI vehicle showing stronger trends than the SG-SIDI vehicle. For the WG-SIDI vehicle, the application of higher alcohol blends led to marked reductions in particle number emissions, which is consistent with previous studies showing a reduced sooting tendency of alcohol fuels due to the presence of oxygen in the fuel [20,21,30,48,51]. The reduction in aromatics content in the fuels may also play some role in decreasing particle number emissions with increasing alcohol content. This is consistent with the findings of Wallner and Frazee [28], which showed that the reduction in the availability of carbon in ethanol combustion decreases the potential for benzene and soot formation as the ethanol blend ratio increases. For the FTP, the weighted particle number emissions showed statistically significant increases of 112%, 120%, and 126%, respectively, for E10, E15, and Bu24 compared to Bu32. The Bu24 and E15 blends showed marginally statistically significant increases of 81% and 77%, respectively, compared to E20. For the cold-start phase of the FTP, particle number emissions showed statistically significant increases of 81% and 66% for Bu24 and 71% and 56% for E15 relative to Bu32 and E20, respectively. E10 showed a marginally statistically significant increase of 57% compared to Bu32. For the hot-running and hot-start phases of the FTP, the ethanol blends and most butanol blends showed statistically significant higher particle number emissions compared to Bu32. For the UC, the weighted particle number emissions resulted in statistically significant

increases of 155%, 145%, and 140%, respectively, for E10, E15, and Bu24 compared to Bu32. No strong fuel trends were seen for the cold-start phase of the UC, while for the hot-running and hot-start phases the ethanol and other butanol blends showed statistically significant increases in particle number emissions compared to Bu32.

Most of the particle emissions occur toward the beginning of the FTP and UC test cycles, as the engine and TWC converter are not yet at operating temperature and therefore particles consisting of volatile residues cannot be effectively oxidized. Fig. 7 displays the real-time traces of particle number and soot emissions over the FTP and gives some insight on their formation mechanism. For comparison purposes, real-time particle number and soot emissions are provided for both vehicles on E10. Interesting trends emerge from the data in Fig. 7, showing that particles are mainly formed during the first 200–300 s of the cycle, which could be due to fuel accumulation onto the cold piston and cylinder surfaces. This phenomenon was more pronounced for the SG-SIDI vehicle, with the cold-start phase dominating the particle number emissions, during which more than approximately 70% of the total emitted particles may be produced. Elevated particle number emissions were also observed during short periods that coincide with vehicle accelerations (i.e., some particle number peaks during sharp accelerations for the hot-start phase). While the WG-SIDI vehicle showed sharp increases in particle number emissions during the cold-start phase, particles were also produced over the entire duration of the cycle and remained relatively high even after engine warm-up. For both vehicles, the vast majority of particles were produced during vehicle accelerations. The more aggressive the acceleration, the higher the concentration of particles produced. It is clear that particle emissions for both vehicles generally decreased after the first 300 s. It is assumed that this is a result of increasing surface temperatures aiding better fuel vaporization and avoiding pool fires. Similar to particle number emissions, soot emissions for both vehicles were dominated by the cold-start phase, with the WG-SIDI vehicle showing significantly higher soot emissions over the entire cycle compared to the SG-SIDI vehicle. Interestingly, soot emissions show that cold-start particles for the SG-SIDI vehicle were primarily organic carbon in nature and that a larger fraction of particles were volatiles when compared with the WG-SIDI vehicle.

3.2.5. Particle size distributions

The transient particle size distributions for the WG-SIDI vehicle and the SG-SIDI vehicle over the FTP and UC are shown in Fig. 8 (a–b). Both vehicles displayed diesel-like distributions and fit well a bimodal lognormal function. For the SG-SIDI vehicle for both test cycles, the number-weighted particle size distribution for all fuels was decidedly bimodal. While the accumulation mode peak dominated the particle size distribution, there is also a nucleation mode present as well. For the SG-SIDI vehicle, the accumulation mode geometric mean particle diameter centered around 35–50 nm for the FTP and 40–50 nm for the UC. The peak particle size of the nucleation mode for the SG-SIDI was about 11 nm in diameter for both cycles. The WG-SIDI vehicle emitted considerably higher concentrations of accumulation mode particles over both test cycles compared to the SG-SIDI vehicle. This can be attributed to the fact that there will be more localized fuel-rich zones in the charge cloud due to the reduced mixture preparation time associated with wall-guided engine architectures. For the WG-SIDI

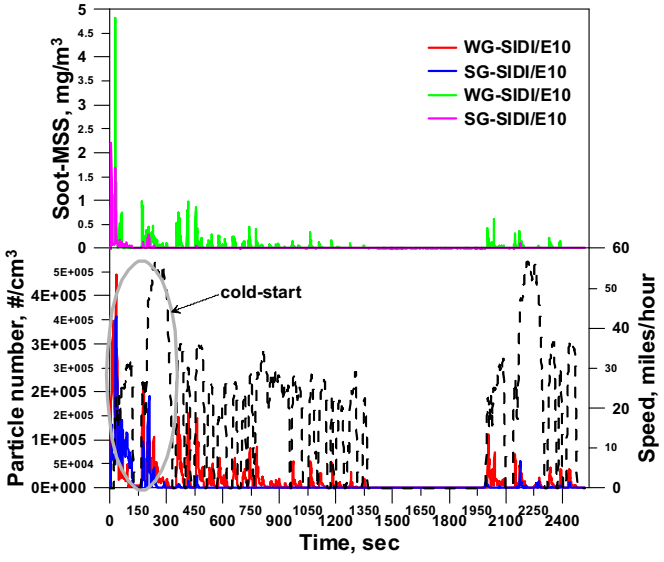

Fig. 7. Real-time soot mass (top panel) and particle number (bottom panel) emissions for the SG-SIDI and WG-SIDI vehicles on E10 over the FTP cycle.

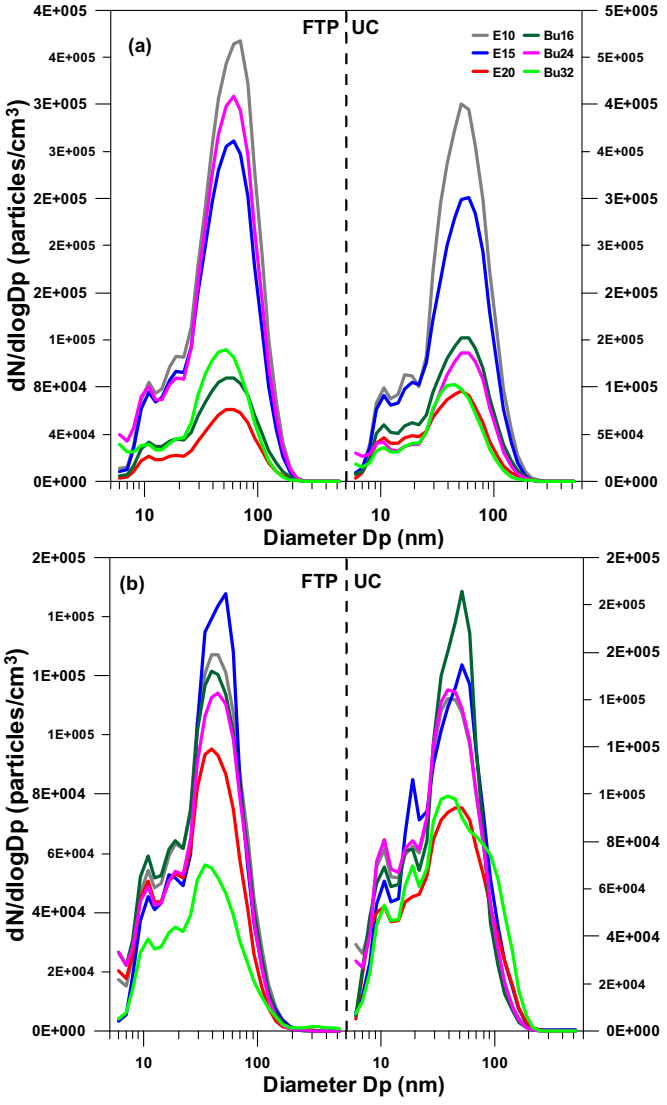

Fig. 8. (a–b): Average particle size distributions for the WG-SIDI vehicle (top panel, a) and SG-SIDI vehicle (bottom panel, b) over the FTP and UC test cycles.

vehicle, the accumulation mode geometric mean particle diameter ranged from 55 to 70 nm for the FTP and from 50 to 60 nm for the UC. Similar to the SG-SIDI vehicle, a nucleation mode distribution with a peak particle size at around 11 nm was seen for the WG-SIDI vehicle over both cycles.

Fuel properties and type seemed to play an essential role in shaping the nature of particle size distributions from SIDI vehicles. For both vehicles, the high oxygen content/low aromatics content fuels resulted in lower number concentration of accumulation mode particles, with this phenomenon being more pronounced for the WG-SIDI vehicle. The higher oxygen/lower aromatic content Bu32 and E20 blends systematically showed lower number concentrations of accumulation mode particles, and in most cases a smaller size in geometric mean diameter compared to the other blends. This is in good agreement with the sharp reductions in soot emissions with the higher ethanol blends, as previously discussed and shown in Fig. 6b. It is assumed that the fuel-bound oxygen in ethanol suppresses soot formation, thus reducing the number of accumulation mode particles. Previous studies in premixed ethanol flames have shown decreases in the amount of soot precursors and a slowdown in the growth process of particles [52,53]. In addition, the water formed by the pyrolysis of ethanol can modify the mechanism of radical formation by decreasing the quantity of soot precursors and the total amount of soot [53]. Note that Bu32 particle size distributions generally shifted towards smaller particle diameters than E20 for both vehicles over both test cycles.

4. Conclusions

This study examined the gaseous and particulate emissions impacts of ethanol and iso-butanol blends for a spray-guided gasoline direct injection vehicle and a wall-guided gasoline direct injection vehicle over the FTP and UC driving cycles using a light-duty chassis dynamometer. Our results showed some reductions in THC and NMHC emissions with increasing alcohol content in the fuel and indicated that these pollutants were largely dominated by the cold-start driving conditions. Emissions of CH_4 and CO_2 also decreased with higher ethanol and butanol blends relative to E10, with some differences being statistically significant. CO emissions generally decreased with higher ethanol blends over the FTP, with some of these differences for the weighted and cold-start CO emissions being statistically significant. The highest reductions in CO emissions were observed for E20 relative to E10, and could be ascribed to the fuel-bound oxygen and the lower T50 of these fuels. For the weighted NO_x emissions, there were no strong fuel trends for either driving cycle for either test vehicle.

Formaldehyde and acetaldehyde were the predominant aldehydes in the tailpipe followed by butyraldehyde, benzaldehyde, propionaldehyde, crotonaldehyde, methacrolein, and hexanaldehyde. Weighted formaldehyde and acetaldehyde emissions did not show strong fuel trends, while statistically significant increases in acetaldehyde emissions were seen for the cold-start phase of the FTP for the higher ethanol and butanol blends relative to E10. An important finding of this study was the statistically significant increase in butyraldehyde emissions with butanol blends compared to ethanol blends. Toluene was the dominant compound in the exhaust followed by benzene and *m/p*-xylene. Monoaromatic emissions decreased with increasing alcohol content in the fuel, with some emission differences being statistically significant.

By increasing the ethanol and butanol blend level, the average PM mass, particle number, and soot mass emissions generally decreased over both cycles for the WG-SIDI vehicle. Our results also showed that particulate reductions can be achieved with low- and mid-level alcohol blends from SIDI vehicles and could help meet the future Tier 3/LEV III emission standards. For both vehicles, the particles were dominated with soot accumulation mode size distributions, with the higher oxygen content/lower aromatics content blends lowering the accumulation mode particle concentrations. The penetration of SIDI vehicles into the U.S. market is expected to continue in the future, and the results of this study suggest that alcohol fuels may prove beneficial in reducing most harmful emissions, especially particulates, while spray-guided DI engine designs can substantially reduce PM mass and number emissions.

Acknowledgments

This study was supported by the California Energy Commission (CEC) under contract 500-09-051 and South Coast Air Quality Management District (SCAQMD) under contract 12208. D. Short was supported under the University of California Transportation Center (UCTC). The authors thank Mr. Kurt Bumiller, Mark Villela, Kevin Castillo, Michelle Ta, and Danny Gomez of the University of California, Riverside for their contribution in conducting the emissions testing for this program.

Appendix A. Supplementary data

Supplementary data related to this article can be found at http://dx.doi.org/10.1016/j.energy.2015.01.023.

References

[1] U.S. Energy Information Administration. Monthly energy review. October 2014. DOE/EIA-0035(2014/10), http://www.eia.gov/totalenergy/data/monthly/pdf/mer.pdf.
[2] Alkidas AC. Combustion advancements in gasoline engines. Energy Convers Manage 2007;48:2751–61.
[3] Zhao F, Lai MC, Harrington D. Automotive spark-ignited direct-injection gasoline engines. Prog Energy Combust Sci 1999;25:437–562.
[4] Stevens E, Steeper R. Piston wetting in an optical DISI engine: fuel films, poolfires, and soot generation. SAE Int J Engines 2001;110:1287–94.
[5] Giglio V, Fiengo G, di Gaeta A, Palladino A. Common rail system for GDI engines. SpringerBriefs in control, automation and robotics. 2013.
[6] Park C, Kim S, Kim H, Moriyoshi Y. Stratified lean combustion characteristics of a spray-guided combustion system in a gasoline direct injection engine. Energy 2012;41:401–7.
[7] Oh H, Bae C. Effects on the injection timing on spray and combustion characteristics in a spray-guided DISI engine under lean-stratified operation. Fuel 2013;107:225–35.
[8] Dahms RN, Drake MC, Fansler TD, Kuo TW, Peters N. Understanding ignition processes in spray-guided gasoline engines using high-speed imaging and the extended spark-ignition model SparkCIMM. Part A: spark channel processes and the turbulent flame front propagation. Combust Flame 2011;158:2229–44.
[9] U.S. Environmental Protection Agency. Fuels and fuel additives, renewable fuel standard, http://www.epa.gov/otaq/fuels/renewablefuels.
[10] European Commission. Directive 2009/30/EC of the European parliament and the council of 23 April 2009 on the promotion of the use of energy from renewable sources and amending and subsequently repealing directives 2001/77/EC and 2003/30/EC. Off J Eur Commun 2009;L140/16.
[11] Gardebroek C, Hernandez MA. Do energy prices stimulate food price volatility? Examining volatility transmission between US oil, ethanol and corn markets. Energy Econ 2013;40:119–29.
[12] Anderson JE, DiCicco DM, Ginder JM, Kramer U, Leone TG, Raney-Pablo HE, Wallington TJ. High octane number ethanol-gasoline blends: quantifying the potential benefits in the United States. Fuel 2012;97:585–94.
[13] Yan X, Inderwildi OR, King DA, Boies AM. Effects of ethanol on vehicle energy efficiency and implications on ethanol life-cycle greenhouse gas analysis. Environ Sci Technol 2013;47:5535–44.
[14] Irimescu A. Performance and fuel conversion efficiency of a spark ignition engine fueled with iso-butanol. Appl Energy 2012;96:477–83.
[15] Jin C, Yao M, Liu H, Lee CFF, Ji J. Progress in the production and application of n-butanol as a biofuel. Renew Sustain Energy Rev 2011;15:4080–106.
[16] Tao L, Tan ECD, McCormick RL, Zhang M, Aden A, He X, Zigler BT. Techno-economic analysis and life-cycle assessment of cellulosic iso-butanol and comparison with cellulosic ethanol and n-butanol. Biofuels Bioprod Biorefin 2014;8:30–48.
[17] Xue C, Zhao XQ, Liu CG, Chen LJ, Bai FW. Prospective and development of butanol as an advanced biofuel. Biotechnol Adv 2013;31:1575–84.

[18] Karavalakis G, Durbin TD, Shrivastava M, Zheng Z, Villela M, Jung H. Impacts of ethanol fuel level on emissions of regulated and unregulated pollutants from a fleet of gasoline light-duty vehicles. Fuel 2012;93:549–58.
[19] Durbin TD, Miller JW, Younglove T, Huai T, Kathalena Cocker. Effects of fuel ethanol content and volatility on regulated and unregulated exhaust emissions for the latest technology gasoline vehicles. Environ Sci Technol 2007;41:4059–64.
[20] Storey JM, Barone T, Norman K, Lewis S. Ethanol blend effects on direct injection spark-ignition gasoline vehicle particulate matter emissions. SAE Int J Fuels Lubr 2010;3:650–9.
[21] Maricq MM, Szente JJ, Jahr K. The impact of ethanol fuel blends on PM emissions from a light-duty GDI vehicle. Aerosol Sci Technol 2012;46:576–83.
[22] Chen L, Stone R, Richardson D. A study of mixture preparation and PM emissions using a direct injection engine with stoichiometric gasoline/ethanol blends. Fuel 2012;96:120–30.
[23] Clairotte M, Adam TW, Zardini AA, Manfredi U, Martini G, Krasenbrink A, Vicet A, Tournie E, Astorga C. Effects of low temperature on the cold start gaseous emissions from light duty vehicles fuelled by ethanol-blended gasoline. Appl Energy 2013;102:44–54.
[24] Price P, Twiney B, Stone R, Kar K, Walmsley H. Particulate and hydrocarbon emissions from a spray guided direct injection spark ignition engine with oxygenated fuel blends. SAE Technical Paper 2007-01-0472.
[25] Graham LA, Belisle SL, Baas CL. Emissions from light duty gasoline vehicles operating on low blend ethanol gasoline and E85. Atmos Environ 2008;42:4498–516.
[26] Schulz M, Clark S. Vehicle emissions and fuel economy effects of 16% butanol and various ethanol blended fuels (E10, E20, and E85). J ASTM Int 2011;8:1–19.
[27] Ratcliff MA, Luecke J, Williams A, Christensen ED, Yanowitz J, Reek A, McCormick RL. Impact of higher alcohols blended in gasoline on light-duty vehicle exhaust emissions. Environ Sci Technol 2013;47:13865–72.
[28] Wallner T, Frazee R. Study of regulated and non-regulated emissions from combustion of gasoline, alcohol fuels and their blends in a DI-SI engine. 2010. SAE Technical Paper 2010-01-1571.
[29] Wallner T, Miers SA, McConnell S. A comparison of ethanol and butanol as oxygenates using a direct-injection, spark-ignition engine. J Eng Gas Turbines Power 2009;131:1–9.
[30] Karavalakis G, Short D, Vu D, Villela M, Asa-Awuku A, Durbin T. Evaluating the regulated emissions, air toxics, ultrafine particles, and black carbon from SI-PFI and SI-DI vehicles operating on different ethanol and iso-butanol blends. Fuel 2014;128:410–21.
[31] Karavalakis G, Short D, Hajbabaei M, Vu D, Villela M, Russell R, Durbin T, Asa-Awuku A. Criteria emissions, particle number emissions, size distributions, and black carbon measurements from PFI gasoline vehicles fuelled with different ethanol and butanol blends. 2013. SAE Technical Paper 2013-01-1147.
[32] Knoll K, West B, Huff S, Thomas J. Effects of mid-level ethanol blends on conventional vehicle emissions. 2009. SAE Technical Paper 2009-01-2723.
[33] Lipman TE, Delucchi MA. Emissions of nitrous oxide and methane from conventional and alternative fuel motor vehicles. Clim Change 2002;53:477–516.
[34] Broustail G, Halter F, Seers P, Moreac G, Mounaim-Rousselle C. Comparison of regulated and non-regulated pollutants with iso-octane/butanol and iso-octane/ethanol blends in a port-fuel injection spark-ignition engine. Fuel 2012;94:251–61.
[35] Schifter I, Diaz L, Rodriguez R, Salazar L. Oxygenated transportation fuels. Evaluation of properties and emission performance in light-duty vehicles in Mexico. Fuel 2011;90:779–88.
[36] U.S. Environmental Protection Agency. Assessing the effect of five gasoline properties on exhaust emissions from light-duty vehicles certified to Tier 2 standards: analysis of data from EPAct phase 3 (EPAct/V2/E-89). Final Repor. April, 2013. t. EPA-420-R-13–002, http://www.epa.gov/otaq/models/moves/epact.htm.
[37] Yanowitz J, Knoll K, Kemper J, Luecke J, McCormick RL. Impact of adaptation on flex-fuel vehicle emissions when fueled with E40. Environ Sci Technol 2013;47:2990–7.
[38] Sarathy SM, Vranckx S, Yasunaga K, Mehl M, Oswald P, Metcalfe WK, Westbrook CK, Pitz WJ, Kohse-Hoinghaus K, Fernandes RX, Curran HJ. A comprehensive chemical kinetic combustion model for the four butanol isomers. Combust Flame 2012;159:2028–55.
[39] Zervas E, Montagne X, Lahaye J. Emission of alcohols and carbonyl compounds from a spark ignition engine. Influence of fuel and air/fuel equivalence ratio. Environ Sci Technol 2002;36:2414–21.
[40] Yasunaga K, Mikajiri T, Sarathy SM, Koike T, Gillespie F, Nagy T, Simmie JM, Curran HJ. A shock tube and chemical kinetic modeling study of the pyrolysis and oxidation of bytanols. Combust Flame 2012;159:2009–27.
[41] Moss JT, Berkowitz AM, Oehlschlaeger MA, Biet J, Warth V, Glaude PA, Battin-Leclerc F. An experimental and kinetic modeling study of the oxidation of the four isomers of butanol. J Phys Chem A 2008;112:10843–55.
[42] Jacobson MZ. Effects of ethanol (E85) versus gasoline vehicles on cancer and mortality in the United States. Environ Sci Technol 2007;41:4150–7.
[43] Carter WPL. Development of the SAPRC-07 chemical mechanism. Atmos Environ 2010;44:5324–35.
[44] Li Y, Xue J, Johnson K, Durbin T, Villela M, Pham L, Hosseini S, Short D, Karavalakis G, Asa-Awuku A, Jung H. Determination of suspended exhaust PM mass for light duty vehicles using IPSD method. 2014. SAE Technical Paper 2014-01-1594.
[45] Zhang S, McMahon W. Particulate emissions for LEV II light-duty gasoline direct injection vehicles. SAE Int J Fuels Lubr 2012;5:637–46.
[46] Piock W, Hoffmann G, Berndorfer A, Salemi P, Fusshoeller B. Strategies towards meeting future particulate matter emission requirements in homogeneous gasoline direct injection engines. SAE Int J Engines 2011;4:1455–68.
[47] Costagliola MA, De Simio L, Iannaccone S, Prati MV. Combustion efficiency and engine out emissions of a S.I. engine fueled with alcohol/gasoline blends. Appl Energy 2013;111:1162–71.
[48] Wang C, Xu H, Herreros JM, Lattimore T, Shuai S. Fuel effect of particulate matter composition and soot oxidation in a direct-injection spark ignition (DISI) engine. Energy Fuels 2014;28:2003–12.
[49] Maricq MM, Szente JJ, Adams J, Tennison P, Rumpsa T. Influence of mileage accumulation on the particle mass and number emissions of two gasoline direct injection vehicles. Environ Sci Technol 2013;47:11890–6.
[50] He X, Ireland JC, Zigler BT, Ratcliff MA, Knoll KE, Alleman TL, Tester JT. The impacts of mid-level biofuel content in gasoline on SIDI engine-out and tailpipe particulate matter emissions. 2010. SAE Technical Paper 2010-01-2125.
[51] Storey JM, Lewis S, Szybist J, Thomas J, Barone T, Eibl M, Nafziger E, Kaul B. Novel characterization of GDI engine exhaust for gasoline and mid-level gasoline-alcohol blends. 2014. SAE Technical Paper 2014-01-1606.
[52] Maricq MM. Soot formation in ethanol/gasoline fuel blend diffusion flames. Combust Flame 2012;159:170–80.
[53] Salamanca M, Sirignano M, Commodo M, Minutolo P, D'Anna A. The effect of ethanol on the particle size distributions in the ethylene premixed flames. Exp Therm Fluid Sci 2012;43:71–5.